

MS-TCT: Multi-Scale Temporal ConvTransformer for Action Detection

Rui Dai^{1,2}, Srijan Das³, Kumara Kahatapitiya³, Michael S. Ryoo³, François Brémond^{1,2}
¹Inria ²Université Côte d’Azur ³Stony Brook University
^{1,2}{name.surname}@inria.fr

Abstract

Action detection is an essential and challenging task, especially for densely labelled datasets of untrimmed videos. The temporal relation is complex in those datasets, including challenges like composite action, and co-occurring action. For detecting actions in those complex videos, efficiently capturing both short-term and long-term temporal information in the video is critical. To this end, we propose a novel ConvTransformer network for action detection. This network comprises three main components: (1) Temporal Encoder module extensively explores global and local temporal relations at multiple temporal resolutions. (2) Temporal Scale Mixer module effectively fuses the multi-scale features to have a unified feature representation. (3) Classification module is used to learn the instance center-relative position and predict the frame-level classification scores. The extensive experiments on multiple datasets, including Charades, TSU and MultiTHUMOS, confirm the effectiveness of our proposed method. Our network outperforms the state-of-the-art methods on all the three datasets.

1. Introduction

Action detection is a popular computer vision problem that aims at finding precise temporal boundaries of actions occurring in an untrimmed video. In real-world videos, every minute is filled with potential actions to be detected and labelled. To depict such challenge, some datasets [8, 35, 45] are densely labelled to have a real-world like action distribution. In these videos, multiple actions can occur concurrently and there is limited background information in the video. To detect the actions in such complex videos, it is important to model both short-term and long-term temporal dependencies of the actions. As shown in figure 1, action instances like *making sandwich* and *opening fridge* can provide context to action instance like *taking food*, which corresponds to the short-term and long-term action dependencies respectively. Also, knowing the occurrence of the action *putting something on the table* and *making sandwich* provides contextual information to detect the composite action *cooking*. This example illustrates that the requirement

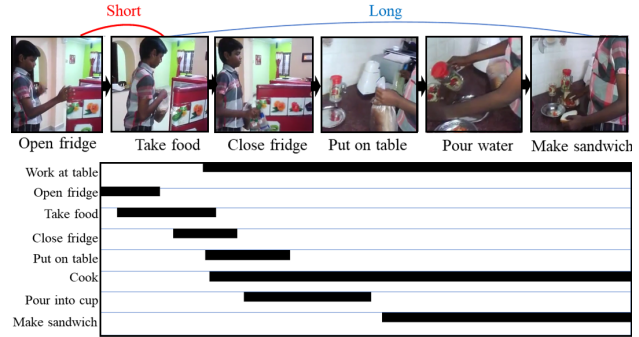


Figure 1. Complex temporal relation. Here, we provide the action distribution in a densely labelled video. Both long-term and short-term action dependencies exist in the video.

of an effective temporal modeling is crucial for detecting actions in a densely labelled video.

Towards modeling temporal relations in untrimmed videos, some methods [7, 9, 10, 25, 33] utilize one-dimensional convolution (i.e., temporal convolutions [25]) to model temporal relations locally. However, limited by the shareable kernel and their kernel size, convolution based methods can not learn direct relations between the distant segments within a video. By segment, we mean a set of consecutive image frames in the video. Thus, these methods fail to model long-range interactions between the segments which may be important for action detection. With the success of transformer [14, 29, 38, 49] in natural language processing and image tasks, recent methods [36, 37] leverage multi-head attention to model the long-term relations in videos for the task of action detection. Such attention mechanisms can build the direct one-to-one global relationship between every temporal segments (i.e. tokens) of the video to detect the highly correlated and composite actions. However, these transformers rely on building a long-term relationship among the input tokens. These tokens are composed of few frames, which is often too short compared to the action instance duration. Thus, temporal consistency between neighboring tokens is important while learning representation for an action instance. But, the pure traditional transformers do not have a specific mechanism to enhance the relation between neighbouring tokens, thus not appropriate for the task of action detection.

To this end, we propose a **Multi-Scale Temporal ConvTransformer (MS-TCT)** taking benefit from both convolution as well as transformer. The functionalities of the convolutions in MS-TCT are: (i) it promotes several temporal scales by performing a weighted pooling of the tokens, thus merging the temporal segments with relevant weighting factor, (ii) it blends the neighboring tokens after a multi-head attention operation to maintain the temporal consistency within an action instance. In a nutshell, MS-TCT is built on top of the temporal segments encoded by a 3D Convolutional Networks [4]. Each temporal segment is treated as input tokens to MS-TCT which processes them in multiple stages at different temporal scales. The temporal scales in MS-TCT are determined by the number of tokens input to each stage of the network. Learning the temporal relations through MS-TCT is done by learning fine-grained relations between atomic actions (e.g. *open fridge*) in the lower stages and learning coarse relations between composite actions (e.g. *cooking*) in the higher stages. Each stage constitutes a temporal convolution for merging the tokens, a set of multi-head attention layer and temporal convolution layer to model global temporal relations and to infuse local information among the tokens respectively. As we know that convolution introduces inductive biases [13], thus temporal convolution layers in MS-TCT infuse positional information related to the tokens [19, 21] without requiring any additional positional embedding unlike what is done for the vision transformers [14]. After modeling temporal relations at different scales, a mixer module is used to fuse the features from different stages to compute a unified representation of the video. To predict the densely distributed actions, besides the multi-label classification branch, we introduce a heat-map branch in MS-TCT. This heat-map encourages the network to predict the relative temporal position of the instances per action class. Figure 2 shows that the relative temporal position is computed by the Gaussian filter based on the instance center and its duration. Each time-step in this heat-map represents the relative temporal position to the action instance center. With this new branch, MS-TCT can embed the class-wise relative temporal position in the token representations, thus it encourages discriminative token classification for complex videos.

To summarize, the main contributions of this work are: 1) We propose an effective and efficient ConvTransformer for modeling complex temporal relations in untrimmed videos. 2) We introduce a new learning branch to learn the position relative to instance-center, which promotes action detection in densely labelled videos. 3) We evaluate our network on three challenging densely labelled action datasets and outperform the state-of-the-art results.

2. Related Work

In this section, we revise the related work of MS-TCT. Action detection has received a lot of interest in recent

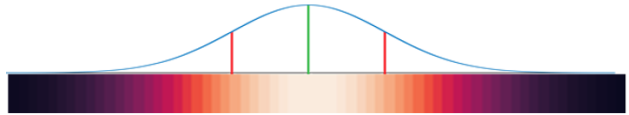


Figure 2. Relative temporal position heat-map (G^*). The heat-map is defined by the center location of the instance (green line), and by its duration (red line).

years [10, 12, 18, 26, 44, 46]. In this work, we focus on action detection in densely labelled videos [8, 35, 45]. The early attempts on modeling complex temporal relations are to use anchor-based methods [5, 43], although dense action distribution requires large amount of anchors. Moreover, the Non-Maximal Suppression post-processing step can not handle such high rate of overlapping actions. Superevent [32] utilizes a set of Gaussian filters to learn the video glimpses. The set of glimpse representations are summed up by a soft attention mechanism to form the global representation of the video. However, the Gaussian filters are independent of the videos, thus the method can not handle videos with minor frequencies of composite actions. Similarly, TGM [33] is a temporal filter whose weights are based on Gaussian distributions. This setting enables TGM to learn longer temporal structures with a limited number of parameters. PDAN [7] is a temporal convolutional network, whose temporal kernels are adaptive to the input data. Although TGM and PDAN achieve state-of-the-art performance in modeling complex temporal relations, these relations are constrained to local regions, thus preventing them to learn long-range relationships. Coarse-Fine Network [23] leverages two X3D [15] networks in a Slow-Fast [16] fashion. This network can model spatio-temporal relations jointly. However, it is limited by the number of input frames to X3D and a large stride is needed for processing long videos. Therefore, Coarse-Fine Network does not take into account the fine-grained details in long videos while detecting action boundaries.

Recent Transformer networks have been successful in both image and video tasks [1, 2, 6, 14, 29, 30, 39, 40, 42, 47, 49]. Although Vision Transformer like TimeSformer [38] can input 96 frames to model temporal relations in short video clips, it is still insufficient to model the fine-grained details in long real-world videos. As a compromise, recent action detection methods use multi-head attention layers on top of the visual segments encoded by 3D Convolutional Network [4]. Among those methods, RTD-Net [36], extended from DETR [49], utilizes the transformer decoder to model the relation between the proposal and the tokens. However, this network is designed only for sparsely annotated videos [3, 22], where a single action exists per video. Because of the dense action distribution, the module that detects the boundaries fails to separate the foreground and background regions in such complex videos. MLAD [37] learns class-specific features and utilizes the transformer encoder to model the class relations for every time-step and

temporal relations for every class. However, such architecture design has hard time to capture the different action class relations across different time-steps. Also, MLAD struggles with datasets that feature complex labels [35], as the class-specific features are hard to extract for those videos. In contrast to these transformers fabricated for action detection, we propose a ConvTransformer called MS-TCT, which inherits the transformer encoder architecture, but also benefits from both temporal convolution and multi-head attention. This network structurally models the temporal tokens globally and locally at different temporal scales. Although other ConvTransformers [13, 19, 41] exist for image classification, our network is redesigned and rooted for densely labelled action detection task.

In the following section, we introduce our proposed network in details.

3. Proposed Network

Firstly, we define the problem statement of action detection in the densely labelled videos. Formally, for a video sequence of length T , each time-step t contains a ground-truth action label $y_{t,c} \in \{0, 1\}$, where $c \in \{1, \dots, C\}$ indicates an action class. For every time-step, an action detection network predicts class probabilities $\hat{y}_{t,c} \in [0, 1]$. In this section, we describe our proposed action detection network: MS-TCT. As depicted in figure 3, this network consists of four main parts: (1) **Visual Encoder** encodes a preliminary video representation, (2) **Temporal Encoder** structurally models the temporal relations at different temporal scales (i.e., resolution), (3) **Temporal Scale Mixer**, dubbed as TS Mixer, combines the multi-scale temporal representation of a video, and (4) **Classification Module** to predict the class probabilities. In the following, we present each of these parts of MS-TCT.

3.1. Visual Encoding

The input to the MS-TCT action detection network is an untrimmed video that can last for a very long duration [8]. Processing long videos in both spatial and temporal dimensions challenge the current computation resources. As a compromise, similar to other action detection models [7, 33, 37], the input to MS-TCT are the features of video segments extracted by a 3D CNN, which embeds spatial information latently within its channels. In this work, we use I3D network [4] to encode the video: Each video is divided into T non-overlapping segments and each segment consists of 8 frames. The input to the I3D network is the RGB images of a segment. Each segment-level feature can be seen as a transformer token of a time-step. We stack the tokens along the temporal axis to form a $T \times D_0$ video representation. Then, the tokens of the video are fed to the Temporal Encoder.

3.2. Temporal Encoder

As discussed earlier in Section 1, efficient temporal modeling is critical for understanding long-term temporal relations of a video, especially for complex action combinations. Given the video tokens, the layers that model the temporal information are of two types: (a) Temporal Convolutional layer [25] is a one dimensional layer across time, which focuses on the neighboring tokens but overlooks their long-term temporal dependencies in the video. (b) Transformer [38] layer that globally encodes the one-to-one interaction for all the tokens, while neglecting the local semantics, which has proven beneficial in modeling the high correlation in visual signals [17, 20]. The Temporal Encoder benefits from both layers to explore both local and global contextual information alternately.

As shown in figure 3, Temporal Encoder follows a hierarchical structure with N stages: Lower stages learn fine-grained action representation with more temporal tokens, whereas higher stages learn coarse action representation with a small number of tokens. Every stage corresponds to a semantic level and consists of one Temporal Merging block and B Global-Local Relational Blocks (see figure 4): **Temporal Merging Block** is the key block for constructing the network hierarchy, which shrinks the number of tokens (i.e., temporal resolution) and increases the feature size. This step can be seen as a weighted pool operation for the neighboring tokens. In practice, we use a single temporal convolutional layer (kernel size k , and stride 2) to half the number of tokens and extend the channel size γ times. For the first stage, since the token number remains the same as the input video (see figure 3), we set stride to 1 for the temporal convolutional layer and project the feature size from D_0 to D .

Global-Local Relational Block: As shown in figure 4, this block is further decomposed to *Global Relational Block* and *Local Relational Block*. In Global Relational Block, we utilize the standard multi-head self-attention layer [38] to model the long-term action dependencies in the video, i.e. modeling the global contextual relations. In Local Relational Block, we utilize a temporal convolutional layer (kernel size k) to enhance the token representation by infusing the contextual information from the neighboring tokens. This enhances the temporal consistency of each token while modeling the short-term temporal information pertaining to an action instance.

In the following, we formulate the computation flow inside the Global-Local Relational Block. For brevity, here, we drop the stage index n . For the block $j \in \{1, \dots, B\}$, the input tokens of the block are $X_j \in \mathbb{R}^{T' \times D'}$. Firstly, the tokens are fed to the multi-head attention layer in Global Relational Block, which consists of H attention heads. For head $i \in \{1, \dots, H\}$, the input X_j is projected to the $Q_{ij} = W_{ij}^Q X_j$, $K_{ij} = W_{ij}^K X_j$ and $V_{ij} = W_{ij}^V X_j$, where $W_{ij}^Q, W_{ij}^K, W_{ij}^V \in \mathbb{R}^{D_h \times D'}$ are the weights of linear layers

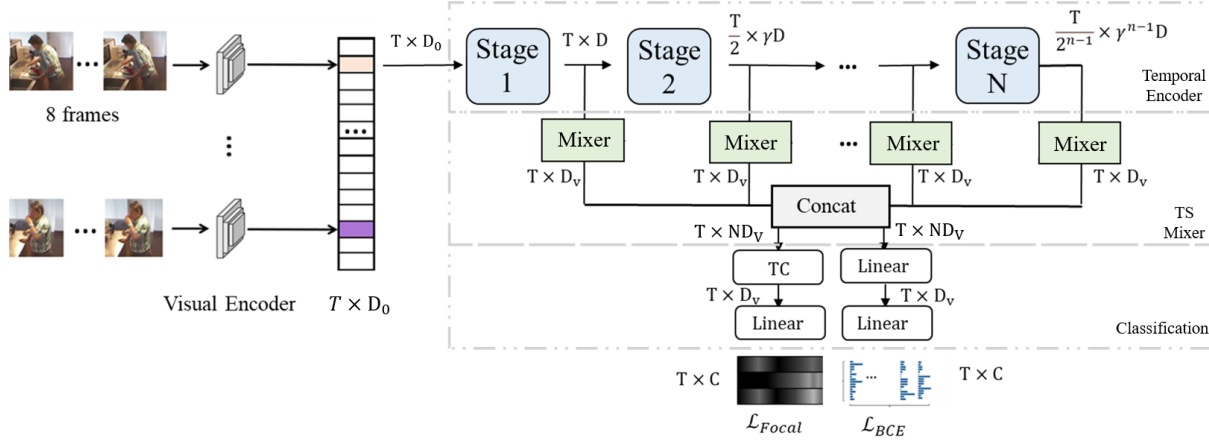


Figure 3. The Multi-Scale Temporal ConvTransformer (MS-TCT) for action detection is composed of four main parts. (1) Visual Encoder, (2) Temporal Encoder, (3) Temporal Scale Mixer (TS Mixer) and (4) Classification Module. Note that TC indicates the 1-dimensional convolutional layer with kernel size k .

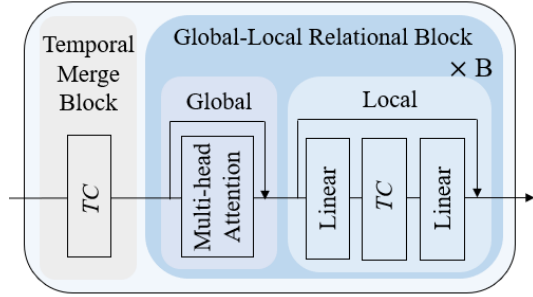


Figure 4. A stage in the Temporal Encoder is composed of (1) Temporal Merging Block (2) B Global-Local Relational Blocks. Each Global-Local Relational Block contains a Global and a Local Relational Block. $Linear$ and TC indicates the 1 dimensional convolutional layer with kernel size 1 and k respectively.

and $D_h = \frac{D'}{H}$ is the feature dimension of the head. Hence, the self-attention for head i is computed as:

$$Att_{ij} = Softmax\left(\frac{Q_{ij}K_{ij}^\top}{\sqrt{D_h}}\right)V_{ij} \quad (1)$$

Then the output of different attention heads are mixed with an additional linear layer as

$$M_j = W_j^O Concat(Att_{1j}, \dots, Att_{Hj}) + X_j \quad (2)$$

where $W_j^O \in \mathbb{R}^{D' \times D'}$ is the weight of the linear layer, the output feature size of multi-head attention layer is same as the input feature size.

Next, the output tokens of multi-head attention are fed to the *Local Relational Block*, which is composed of two linear layers and a temporal convolutional layer. As shown in figure 4, the tokens are first fed to a linear layer to extend the feature dimension from D' to $\theta D'$. Then, a temporal convolutional layer with kernel size k blends the neighboring tokens in a higher dimension and provides the temporal

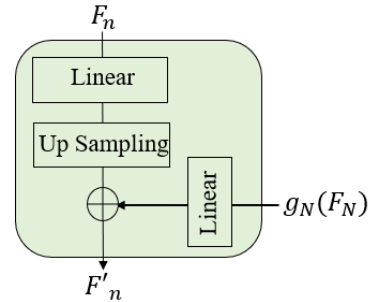


Figure 5. Temporal Scale Mixer Module. The output tokens F_n of stage n is resized and up-sampled to $T \times D_v$, then added with the tokens from the last stage N .

position information to the temporal tokens [21]. After that, another linear layer projects the feature dimension back to D' . The two linear layers in this block enable the transition between the multi-head attention layer and temporal convolutional layer. The output feature dimension remains the same as the input feature for the Local Relational Block. This output is fed to the next Global Relational Block if block $j < B$.

The output tokens from the last Global-Local Relational Block from each stage are combined and fed to the following Temporal Scale Mixer.

3.3. Temporal Scale Mixer

After obtaining the tokens at different temporal scales, the question that remains, *how to aggregate these tokens to have a unified video representation?* In order to predict the action probabilities, the classification module needs to predict on the original temporal length as the network input. Thus, we require to interpolate the tokens across the temporal dimension which is achieved by performing an up-sampling and a linear operation. As shown in figure 5, for

the output F_n from stage $n \in \{1, \dots, N\}$, the operation is formulated as:

$$g_n(F_n) = \text{UpSampling}_n(F_n W^n) \quad (3)$$

where $W^n \in \mathbb{R}^{D_v \times \gamma^{n-1} D}$ and up sampling rate is n . As in our hierarchical architecture, the shallower stages (i.e. low semantics) represents higher temporal scales, while the deeper stages (i.e. high semantics) represents lower temporal scales. To balance the resolution and semantics, the up-sampled tokens from the last stage N is processed by a linear layer and added with the up-sampled tokens of each stage ($n < N$). The operation can be formulated as:

$$F'_n = g_n(F_n) \oplus g_N(F_N) W_n \quad (4)$$

where F'_n is the refined tokens of stage n , \oplus indicates the element-wise addition and $W_n \in \mathbb{R}^{D_v \times D_v}$. Then all the refined tokens are having the same length. They are concatenated to have the final multi-scale video representation $F_v \in \mathbb{R}^{T \times N D_v}$.

$$F_v = \text{Concat}(F'_1, \dots, F'_{N-1}, F'_N) \quad (5)$$

Note that more complicated fusion methods [11, 28] could be built on top of these tokens from different stages. However, our attempts have not shown further improvement.

The multi-scale video representation F_v is then sent to the classification module for succeeding predictions.

3.4. Classification Module

Training MS-TCT is achieved by jointly learning two classification tasks. As mentioned in section 1, in this work, we introduce a new classification branch to learn a heat-map of the action instances. This heat-map is different from the ground truth label as it varies across time based on the action center and action duration. The objective of using such heat-map representation is to encode temporal relative positioning to the learned tokens of MS-TCT.

In order to train the heat-map branch, we need first to build the class-wise ground-truth heat-map response $G^* \in [0, 1]^{T \times C}$, where C indicates the number of action classes. In this work, we construct G^* by considering the maximum response of a set of one-dimensional Gaussian filters. Each Gaussian filter corresponds to an instance of a class in a video, centered at the action instance in the video. More precisely, for every temporal location t the ground-truth heat-map response is formulated as:

$$G_c^*(t) = \max_{a=1, \dots, A_c} \text{Gaussian}(t, t_{a,c}; \sigma) \quad (6)$$

$$\text{Gaussian}(t, t_{a,c}; \sigma) = \frac{1}{\sqrt{2\pi}\sigma} \exp\left(-\frac{(t-t_{a,c})^2}{2\sigma^2}\right) \quad (7)$$

$\text{Gaussian}(\cdot, \cdot; \sigma)$ provides an instance-specific Gaussian activation according to the center and instance duration. Here, σ is equal to $\frac{1}{2}$ of each instance duration and $t_{a,c}$ is the center for class c and instance a . A_c is the total number of

instances for class c in the video. As shown in figure 3, heat-map G is computed by a temporal convolutional layer with kernel size k and non-linear activation, along with another linear layer with sigmoid activation. Given the ground-truth G^* and the predicted heat-map G , we compute the action focal loss [27, 48] which is formulated as:

$$\mathcal{L}_{Focal} = \frac{1}{A} \sum_{t,c} \begin{cases} (1 - G_{t,c})^2 \log(G_{t,c}) & \text{if } G_{t,c}^* = 1 \\ (1 - G_{t,c}^*)^4 (G_{t,c})^2 \log(1 - G_{t,c}) & \text{Otherwise} \end{cases} \quad (8)$$

where A is the total number of action instances in a video.

Similar to the previous work [7, 37], we leverage another branch to perform the multi-label classification. With video features F_v , the predicted scores are computed by two linear layers with a sigmoid activation. The Binary Cross Entropy (BCE) loss [31] is computed by the predict scores and the ground-truth labels. The scores predicted from this branch are only used for the evaluation. The same output tokens F_v are fed to both branches. The heat-map branch encourages the model to embed the relative position to the instance center into video tokens F_v . Consequently, the classification branch can also benefit from such position information to better classify the tokens.

In summary, the overall loss is formulated as the weighted sum of two losses, the weight α is chosen according to the numerical scale of the loss.

$$\mathcal{L}_{Total} = \mathcal{L}_{BCE} + \alpha \mathcal{L}_{Focal} \quad (9)$$

4. Experiments

Datasets: For experimental analysis, we evaluate our framework on three popular multi-label action detection datasets: Charades [35], TSU [8] and MultiTHUMOS [45]. Charades [35] is a large dataset with 9848 videos of daily indoor actions. The dataset contains 66K+ temporal annotations for 157 action classes, with a high overlap across action instances of different classes. This is in contrast to other action detection datasets such as ActivityNet [3], which only have one action per time-step. We evaluate on the localization setting of the dataset [34]. Similar to the Charades, TSU [8] is also recorded indoor environment with dense annotation. Up to 5 actions can happen at the same time at a frame. Different from Charades, TSU has many long-term composite actions. MultiTHUMOS [45] is an extended version of THUMOS'14 [22], containing dense, multi-label action annotations for 65 classes across the 413 sports videos. By default, we evaluate the per-frame mAP on these densely labeled datasets following [34, 45].

Implementation Details: In the proposed network, the total stage N is set to 4 and the number of Global-Local Relational Block B is set to 3 for each stage. Note that for the small dataset as MultiTHUMOS, 2 blocks are enough. The number of heads for the Global Relational Block is 8. The feature input to MS-TCT are the I3D features extracted from the Global Average Pooling layer and thus,

D_0 is 1024. The input feature is then projected to $D = 256$ dimensional feature by the temporal merging block in the first stage. The feature expansion rate γ and θ are 1.5 and 8 respectively. Kernel size k of temporal convolutional layer is 3, the zero padding rate is 1 to keep the same resolution. The loss balance factor α is 0.05. The number of tokens is fixed to $T = 256$ as input to MS-TCT. For the training phase, we randomly take consecutive T tokens. For the inference phase, we follow [37] to use sliding window approach for the prediction. Our model is trained on two GTX 1080 Ti GPU with a batch-size of 32. We use Adam optimizer [24] with an initial learning rate of 0.0001, and we scale it by a factor of 0.5 with a patience of 8 epochs.

4.1. Ablation Study

In this section, we study the effectiveness of each component in the proposed network on the Charades dataset.

Table 1. Ablation study for the components in MS-TCT. The evaluation is based on per-frame mAP on Charades dataset using RGB videos.

Temporal Encoder	TS Mixer	Heat-Map Branch	Classification Branch	mAP (%)
×	×	×	✓	15.6
✓	×	×	✓	23.6
✓	✓	×	✓	24.1
✓	✓	✓	×	10.7
✓	✓	✓	✓	25.4

Importance of Each Component in MS-TCT. As shown in Table 1, I3D features with only the classification branch is considered as the representative baseline. This baseline network consists in a classifier that discriminates the I3D features at each time-step without any further temporal modeling. On top of that, adding the temporal encoder significantly improves the performance (+ 7.0%) w.r.t. I3D feature baseline. This improvement reflects the effectiveness of the temporal encoder in modeling the temporal relations within the videos. Then, in addition to the temporal encoder, we introduce a Temporal Scale Mixer to blend the features from different temporal scales, which introduces + 0.5% improvement, with limited additional computation cost. Finally, we study the usage of the heat-map branch in the classification module. We find that the heat-map branch is effective when optimized in addition to the classification branch, but fails to learn discriminative representation when optimized without the classification branch (25.4% vs 10.7%). The heat-map branch encourages the tokens to predict the action center while minor the tokens on the action boundaries. In comparison, the classification branch improves the token representation equally for all tokens between action boundaries. Thus, both branches when optimized together, enable the model to learn a complete action representation. While having all the components, the proposed network achieves + 9.8% improvement w.r.t. I3D

Table 2. Ablation study for the design choice of a stage in the Temporal Encoder. The evaluation is based on per-frame mAP on Charades dataset.

Temporal Merge	Global Layer	Local Layer	mAP (%)
✓	✓	×	24.0
✓	×	✓	20.9
×	✓	✓	22.7
✓	✓	✓	25.4

feature baseline corroborating that each component in MS-TCT is instrumental for the task of action detection.

Design Choice for a Stage. In Table 2, we present the ablation for the design choice of the stage(s) of the temporal encoder. Each row in Table 2 indicates the result of removing a component in the stage. Note that, removing the temporal merge block indicates replacing this block with a temporal convolutional layer of stride 1, i.e., only the channel dimension is modified across stages. In Table 2, we find that ablating any component can drop down the network performance with a large margin. This observation shows the importance of jointly modeling both global and local relations in the network and the importance of multi-scale structure. These properties in MS-TCT make it easier to learn complex temporal relationships that exist across (i) the neighboring temporal segments, and (ii) the distant temporal segments.

Analysis of the Local Relational Block. Finally, we dig deeper into the Local Relational Block in one stage. As shown in figure 4, there are two linear layers and one temporal convolutional layer in the Local Relational Block. In Table 3, we further perform ablations of these components. Firstly, we find that without the temporal convolutional layer, the action detection performance drops down. This observation shows the importance of mixing the transformer tokens with a temporal locality. Secondly, we study the importance of the transition layer (i.e., linear layer). When the feature size remains constant, having the transition layer can boost the performance by + 1.8%, which shows the importance of such transition layers. Finally, we study how the expansion rate affects the network performance. While setting different feature expansion rates, we find that temporal convolution can better model the local temporal relations when the input feature is in a higher dimensional space.

4.2. Comparison to the State-of-the-Art

In this section, we compare MS-TCT with the state-of-the-art action detection methods (see Table 4). Proposal based methods, such as R-C3D [43] fail in multi-label datasets due to the high overlapping rate of action instances, which challenges the proposal and NMS-based methods. Superevent [32] superposes a global representation to each local feature based on a series of learnable temporal filters. However, the distribution of actions varies from one video

Table 3. Ablation study inside the Local Relational Block on Charades. The evaluation is based on per-frame mAP using RGB. \times indicates we remove the linear or temporal convolutional layer. Feature expansion rate 1 indicates that the feature-size is not changed in the Local Relational Block.

Feature Expansion Rate (θ)	Temporal Convolution	mAP (%)
8	\times	22.3
\times	\checkmark	22.4
1	\checkmark	24.2
4	\checkmark	24.9
8	\checkmark	25.4

Table 4. Comparison with the state-of-the-art methods on three densely labelled datasets. Backbone indicates the visual encoder. Note that the evaluation for the methods is based on per-frame mAP (%) using only RGB videos.

	Backbone	GFLOPs	Charades	MultiTHUMOS	TSU
R-C3D [43]	C3D	-	12.7	-	8.7
Super-event [32]	I3D	0.8	18.6	36.4	17.2
TGM [33]	I3D	1.2	20.6	37.2	26.7
PDAN [7]	I3D	3.2	23.7	40.2	32.7
Coarse-Fine [23]	X3D	-	25.1	-	-
MLAD [37]	I3D	44.8	18.4	42.2	-
MS-TCT	I3D	6.6	25.4	43.1	33.7

to the other. As super-event learns a fixed filter location for all the videos in the training distribution, this location is suitable to mainly actions with high frequency. TGM [33] and PDAN [7] are methods based on temporal convolution of video segments. Nevertheless, those methods only process videos locally in a single temporal scale. Thus, they are not effective in modeling long-term dependencies and high-level semantics. Coarse-Fine Network [23] achieves 25.1% on Charades. However, this method is built upon the video encoder X3D [15], which prevents using a high number of input frames. Moreover, it relies on a large stride between the frames. Therefore, it fails to model fine-grained action relations and hence can not process long videos in MultiTHUMOS and TSU. MLAD [37] jointly models action class relations for every time-step and temporal relations for every class. This design leads to a huge computational cost while under performing on datasets with a large number of action classes (e.g. Charades). Thanks to the combination of transformer and convolution in a multi-level hierarchy, the proposed MS-TCT consistently outperforms all the state-of-the-art methods on the three multi-label action detection datasets. We also compare the FLOPs computation for the methods build on top of the Visual Encoder (i.e., I3D features), taking as input the same batch of data. We observe that the FLOPs of MS-TCT is higher in a reasonable margin than pure convolutional methods (i.e., PDAN, TGM, super-event). However, compared to a transformer based action detection method MLAD, MS-TCT utilizes only $\frac{1}{7}$ of the FLOPs.

We also evaluate our network with the action-conditional

metrics [37] on Charades dataset in Table 5. This metric is used to measure a method’s ability to model both co-occurrence dependencies and temporal dependencies of action classes. Although our network is not specifically designed to model the cross-class relations as in MLAD, still our method achieves higher performance on all action-conditional metrics with a large margin, showing that MS-TCT effectively models action dependencies both within a time-step (i.e., co-occurring action, $\tau = 0$) and throughout the temporal dimension ($\tau > 0$).

Finally, we present a qualitative evaluation for PDAN and MS-TCT on the Charades dataset in figure 6. As the prediction of the Coarse-Fine network is similar to the X3D network which is limited to dozens of frames, thus we can not compare with the Coarse-Fine network on the whole video. From figure 6, we find that MS-TCT can predict more precisely the action instances than PDAN. This comparison reflects the effectiveness of the transformer architecture and multi-scale temporal modeling.

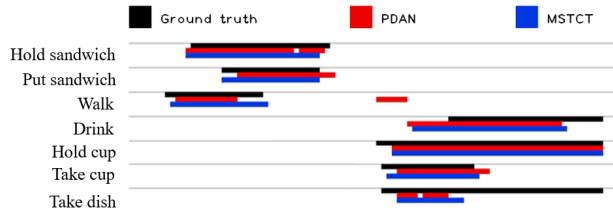


Figure 6. Visualization of the detection results on an example video along time axis. In this figure, we visualize the ground truth and the detection of PDAN and MS-TCT.

4.3. Discussion and Analysis

Transformer, Convolution or ConvTransformer? To confirm the effectiveness of the ConvTransformer, we construct a pure transformer network and a pure convolution network. Each network has the same number of stages as MS-TCT with similar settings (e.g., blocks, feature dimension). Therefore, for pure transformer: a pooling layer and a linear layer constitute the temporal merging block, then B transformer blocks follow in each stage. A transformer block is composed of a multi-head attention layer, norm-add operations and a feed-forward layer. The learned position embedding is added to the input tokens to encode the positional information. The pure transformer architecture achieves 22.3% on Charades. For pure convolution: we retain the same temporal merging block as in MS-TCT, followed by stacking B temporal convolution blocks. Each block is composed of a kernel-sized k temporal convolution layer, a linear layer, a non-linear activation and a residual link. The pure temporal convolution architecture achieves 21.4% on Charades. The proposed ConvTransformer-based method outperforms both the pure transformer and the pure convolution network by a large margin (+ 3.1%, and + 4.0% on Charades, see table 6). This reflects that ConvTransformer can better model the temporal relations of complex

Table 5. Evaluation on the Charades dataset using the action-conditional metrics [37]. Similar to MLAD, both RGB and Optical flow are used for the evaluation. P_{AC} - Action-Conditional Precision, R_{AC} - Action-Conditional Recall, $F1_{AC}$ - Action-Conditional F1-Score, mAP_{AC} - Action-Conditional Mean Average Precision. τ indicates the temporal window size. $\tau = 0$ corresponds to the actions occurring at the same time.

	$\tau = 0$				$\tau = 20$				$\tau = 40$			
	P_{AC}	R_{AC}	$F1_{AC}$	mAP_{AC}	P_{AC}	R_{AC}	$F1_{AC}$	mAP_{AC}	P_{AC}	R_{AC}	$F1_{AC}$	mAP_{AC}
I3D	14.3	1.3	2.1	15.2	12.7	1.9	2.9	21.4	14.9	2.0	3.1	20.3
CF	10.3	1.0	1.6	15.8	9.0	1.5	2.2	22.2	10.7	1.6	2.4	21.0
MLAD [37]	19.3	7.2	8.9	28.9	18.9	8.9	10.5	35.7	19.6	9.0	10.8	34.8
MS-TCT	26.3	15.5	19.5	30.7	27.6	18.4	22.1	37.6	27.9	18.3	22.1	36.4

Table 6. Study on stage type.

Stage-Type	mAP
Pure Transformer	22.3
Pure Convolution	21.4
ConvTransformer	25.4

Table 7. Study on σ .

Variance: σ	mAP
1/8 duration	24.6
1/4 duration	24.8
1/2 duration	25.4

actions.

Heat-map Analysis. We visualize the ground truth heat-map (G^*) and the corresponding prediction heat-map (G) in figure 7. We observe that with the heat-map branch, MS-TCT predicts the center location of the action instances, showing that MS-TCT embeds the center-relative information to the tokens. However, as we optimized with focal loss to highlight the center, the boundaries of the action instance in this heat-map are less visible. We then study the impact of σ to the model performance. As shown in table 7, we set σ to $\frac{1}{8}$, $\frac{1}{4}$ and $\frac{1}{2}$ of the instance duration while generating the ground-truth heat-map G^* . MS-TCT improves by +0.5%, +0.7%, +1.3% respectively w.r.t. the MS-TCT without the heat-map branch, with G^* set to different σ . This result reflects that a larger σ can better provide the center-relative position. We also add heat-map branch to another action detection model: PDAN [7]. Although the heat-map branch also improves PDAN (+0.4%), the relative improvement is much less compared to MS-TCT (+1.3%). MS-TCT features a multi-stage fashion along with a TS Mixer. As the heat-map branch takes input from all the stages, thus, the center-relative position is embedded in an early stage. These tokens with the relative position information when fed to the following stages, the multi-head attention layers is benefited from such additional information to better model temporal relation across the tokens. This design makes MS-TCT to better leverage the heat-map branch than PDAN.

Number of Tokens T . As mentioned in the implementation details, we randomly select consecutive T tokens for each video in the training phase and utilize the sliding window at inference. Here, we have studied how the number of tokens T affects the action detection performance. When T is set to 128, 256 and 512 tokens, MS-TCT achieves 25.0%, 25.4% and 25.5% on Charades. There is no significant difference in the action detection performance while changing the number of input tokens. However, increasing the number of tokens T in MS-TCT increases the FLOPs. For the trade-off between the computation cost and performance precision, we set T to 256 tokens, which corresponds to

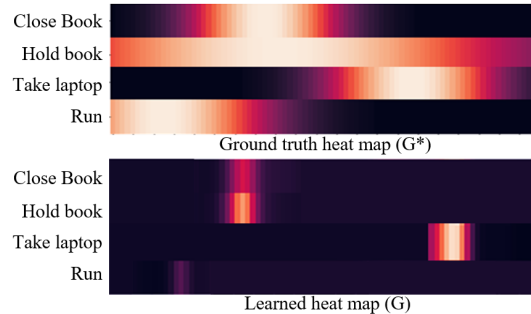


Figure 7. Heat-map visualization along time axis. On the top, we show the ground truth heat-map (G^*) of the example video. On the bottom is the corresponding learned heat-map (G) of MS-TCT. As the heat-map is generated by a Gaussian function, the lighter region indicates closer to the center of the instance.

2048 frames (about 86 sec.) of video.

Temporal Positional Embedding. We study whether Temporal Encoder of MS-TCT requires positional embedding. We find that the performance drops by 0.2% on Charades when a learnable positional embedding [14] is added to the input tokens before processing them into the Temporal Encoder. This shows that the current design can provide the temporal positioning of the tokens. Adding further positional information to the tokens is redundant, leading to lower detection performance.

Method Limitation. Although MS-TCT has outperformed state-of-the-art methods on three challenging datasets, the performance is still relatively low (e.g., less than 30% on Charades). One of the reasons is that the Visual Encoder and the Temporal Encoder in MS-TCT are not optimized jointly in our network, due to hardware limitation. Our future work will focus on modeling the temporal and spatial relations end-to-end for long untrimmed videos.

5. Conclusion

In this work, we propose a novel ConvTransformer network MS-TCT for action detection. This network can model temporal relations both globally and locally at different temporal scales. Moreover, we introduce a new learning branch to learn the class-wise relative position of the action instance center. MS-TCT is evaluated on three challenging densely labelled datasets and outperforms state-of-the-art methods on all of them.

References

- [1] Anurag Arnab, Mostafa Dehghani, Georg Heigold, Chen Sun, Mario Lučić, and Cordelia Schmid. Vivit: A video vision transformer. *arXiv preprint arXiv:2103.15691*, 2021. [2](#)
- [2] Gedas Bertasius, Heng Wang, and Lorenzo Torresani. Is space-time attention all you need for video understanding? *arXiv preprint arXiv:2102.05095*, 2021. [2](#)
- [3] Fabian Caba Heilbron, Victor Escorcia, Bernard Ghanem, and Juan Carlos Niebles. Activitynet: A large-scale video benchmark for human activity understanding. In *Proceedings of the IEEE Conference on Computer Vision and Pattern Recognition*, pages 961–970, 2015. [2](#), [5](#)
- [4] Joao Carreira and Andrew Zisserman. Quo vadis, action recognition? a new model and the kinetics dataset. In *2017 IEEE Conference on Computer Vision and Pattern Recognition (CVPR)*, pages 4724–4733. IEEE, 2017. [2](#), [3](#)
- [5] Guang Chen, Can Zhang, and Yuexian Zou. Afnet: Temporal locality-aware network with dual structure for accurate and fast action detection. *IEEE Transactions on Multimedia*, 2020. [2](#)
- [6] Bowen Cheng, Alexander G Schwing, and Alexander Kirillov. Per-pixel classification is not all you need for semantic segmentation. *arXiv preprint arXiv:2107.06278*, 2021. [2](#)
- [7] Rui Dai, Srijan Das, Luca Minciullo, Lorenzo Garattoni, Gianpiero Francesca, and Francois Bremond. Pdan: Pyramid dilated attention network for action detection. In *Proceedings of the IEEE/CVF Winter Conference on Applications of Computer Vision (WACV)*, pages 2970–2979, January 2021. [1](#), [2](#), [3](#), [5](#), [7](#), [8](#)
- [8] Rui Dai, Srijan Das, Saurav Sharma, Luca Minciullo, Lorenzo Garattoni, Francois Bremond, and Gianpiero Francesca. Toyota smarhome untrimmed: Real-world untrimmed videos for activity detection. *arXiv preprint arXiv:2010.14982*, 2020. [1](#), [2](#), [3](#), [5](#)
- [9] Rui Dai, Luca Minciullo, Lorenzo Garattoni, Gianpiero Francesca, and François Bremond. Self-attention temporal convolutional network for long-term daily living activity detection. In *2019 16th IEEE International Conference on Advanced Video and Signal Based Surveillance (AVSS)*, pages 1–7. IEEE, 2019. [1](#)
- [10] Xiyang Dai, Bharat Singh, Joe Yue-Hei Ng, and Larry Davis. Tan: Temporal aggregation network for dense multi-label action recognition. In *2019 IEEE Winter Conference on Applications of Computer Vision (WACV)*, pages 151–160. IEEE, 2019. [1](#), [2](#)
- [11] Yimian Dai, Fabian Gieseke, Stefan Oehmcke, Yiquan Wu, and Kobus Barnard. Attentional feature fusion. In *Proceedings of the IEEE/CVF Winter Conference on Applications of Computer Vision*, pages 3560–3569, 2021. [5](#)
- [12] Dima Damen, Hazel Doughty, Giovanni Maria Farinella, Sanja Fidler, Antonino Furnari, Evangelos Kazakos, Davide Moltisanti, Jonathan Munro, Toby Perrett, Will Price, and Michael Wray. Scaling egocentric vision: The epic-kitchens dataset. In *European Conference on Computer Vision (ECCV)*, 2018. [2](#)
- [13] Stéphane d’Ascoli, Hugo Touvron, Matthew Leavitt, Ari Morcos, Giulio Biroli, and Levent Sagun. Convit: Improving vision transformers with soft convolutional inductive biases. *arXiv preprint arXiv:2103.10697*, 2021. [2](#), [3](#)
- [14] Alexey Dosovitskiy, Lucas Beyer, Alexander Kolesnikov, Dirk Weissenborn, Xiaohua Zhai, Thomas Unterthiner, Mostafa Dehghani, Matthias Minderer, Georg Heigold, Sylvain Gelly, et al. An image is worth 16x16 words: Transformers for image recognition at scale. *arXiv preprint arXiv:2010.11929*, 2020. [1](#), [2](#), [8](#)
- [15] Christoph Feichtenhofer. X3d: Expanding architectures for efficient video recognition, 2020. [2](#), [7](#)
- [16] Christoph Feichtenhofer, Haoqi Fan, Jitendra Malik, and Kaiming He. Slowfast networks for video recognition. *CoRR*, abs/1812.03982, 2018. [2](#)
- [17] Kunihiko Fukushima. Cognitron: A self-organizing multi-layered neural network. *Biological cybernetics*, 20(3):121–136, 1975. [3](#)
- [18] Joshua Gleason, Rajeev Ranjan, Steven Schwarcz, Carlos Castillo, Jun-Cheng Chen, and Rama Chellappa. A proposal-based solution to spatio-temporal action detection in untrimmed videos. In *2019 IEEE Winter Conference on Applications of Computer Vision (WACV)*, pages 141–150. IEEE, 2019. [2](#)
- [19] Jianyuan Guo, Kai Han, Han Wu, Chang Xu, Yehui Tang, Chunjing Xu, and Yunhe Wang. Cmt: Convolutional neural networks meet vision transformers. *arXiv preprint arXiv:2107.06263*, 2021. [2](#), [3](#)
- [20] David H Hubel and Torsten N Wiesel. Receptive fields, binocular interaction and functional architecture in the cat’s visual cortex. *The Journal of physiology*, 160(1):106–154, 1962. [3](#)
- [21] Md Amirul Islam, Sen Jia, and Neil DB Bruce. How much position information do convolutional neural networks encode? *arXiv preprint arXiv:2001.08248*, 2020. [2](#), [4](#)
- [22] Yu-Gang. Jiang, Jingen Liu, Amir Roshan Zamir, George Toderici, Ivan Laptev, Mubarak Shah, and Rahul Sukthankar. THUMOS challenge: Action recognition with a large number of classes. <http://crcv.ucf.edu/THUMOS14/>, 2014. [2](#), [5](#)
- [23] Kumara Kahatapitiya and Michael S Ryoo. Coarse-fine networks for temporal activity detection in videos. In *Proceedings of the IEEE/CVF Conference on Computer Vision and Pattern Recognition*, pages 8385–8394, 2021. [2](#), [7](#)
- [24] Diederik P. Kingma and Jimmy Ba. Adam: A method for stochastic optimization. *CoRR*, abs/1412.6980, 2014. [6](#)
- [25] Colin Lea, Michael D Flynn, Rene Vidal, Austin Reiter, and Gregory D Hager. Temporal convolutional networks for action segmentation and detection. In *proceedings of the IEEE Conference on Computer Vision and Pattern Recognition*, pages 156–165, 2017. [1](#), [3](#)
- [26] Tianwei Lin, Xu Zhao, and Zheng Shou. Single shot temporal action detection. In *Proceedings of the 25th ACM international conference on Multimedia*, pages 988–996. ACM, 2017. [2](#)
- [27] Tsung-Yi Lin, Priya Goyal, Ross Girshick, Kaiming He, and Piotr Dollár. Focal loss for dense object detection. In *Proceedings of the IEEE international conference on computer vision*, pages 2980–2988, 2017. [5](#)
- [28] Shu Liu, Lu Qi, Haifang Qin, Jianping Shi, and Jiaya Jia. Path aggregation network for instance segmentation. In *Proceedings of the IEEE conference on computer vision and pattern recognition*, pages 8759–8768, 2018. [5](#)

- [29] Ze Liu, Yutong Lin, Yue Cao, Han Hu, Yixuan Wei, Zheng Zhang, Stephen Lin, and Baining Guo. Swin transformer: Hierarchical vision transformer using shifted windows. *arXiv preprint arXiv:2103.14030*, 2021. [1](#), [2](#)
- [30] Ze Liu, Jia Ning, Yue Cao, Yixuan Wei, Zheng Zhang, Stephen Lin, and Han Hu. Video swin transformer. *arXiv preprint arXiv:2106.13230*, 2021. [2](#)
- [31] Jinseok Nam, Jungi Kim, Eneldo Loza Mencía, Iryna Gurevych, and Johannes Fürnkranz. Large-scale multi-label text classification—revisiting neural networks. In *Joint european conference on machine learning and knowledge discovery in databases*, pages 437–452. Springer, 2014. [5](#)
- [32] AJ Piergiovanni and Michael S Ryoo. Learning latent super-events to detect multiple activities in videos. In *Proceedings of the IEEE Conference on Computer Vision and Pattern Recognition*, 2018. [2](#), [6](#), [7](#)
- [33] AJ Piergiovanni and Michael S Ryoo. Temporal gaussian mixture layer for videos. *International Conference on Machine Learning (ICML)*, 2019. [1](#), [2](#), [3](#), [7](#)
- [34] Gunnar A Sigurdsson, Santosh Divvala, Ali Farhadi, and Abhinav Gupta. Asynchronous temporal fields for action recognition. In *Proceedings of the IEEE Conference on Computer Vision and Pattern Recognition*, pages 585–594, 2017. [5](#)
- [35] Gunnar A. Sigurdsson, Gül Varol, Xiaolong Wang, Ali Farhadi, Ivan Laptev, and Abhinav Gupta. Hollywood in homes: Crowdsourcing data collection for activity understanding. In *European Conference on Computer Vision (ECCV)*, 2016. [1](#), [2](#), [3](#), [5](#)
- [36] Jing Tan, Jiaqi Tang, Limin Wang, and Gangshan Wu. Relaxed transformer decoders for direct action proposal generation. *arXiv preprint arXiv:2102.01894*, 2021. [1](#), [2](#)
- [37] Praveen Tirupattur, Kevin Duarte, Yogesh Rawat, and Mubarak Shah. Modeling multi-label action dependencies for temporal action localization. *Proceedings of the IEEE/CVF Conference on Computer Vision and Pattern Recognition*, 2021. [1](#), [2](#), [3](#), [5](#), [6](#), [7](#), [8](#)
- [38] Ashish Vaswani, Noam Shazeer, Niki Parmar, Jakob Uszkoreit, Llion Jones, Aidan N Gomez, Łukasz Kaiser, and Illia Polosukhin. Attention is all you need. In *Advances in neural information processing systems*, pages 5998–6008, 2017. [1](#), [2](#), [3](#)
- [39] Wenhai Wang, Enze Xie, Xiang Li, Deng-Ping Fan, Kaitao Song, Ding Liang, Tong Lu, Ping Luo, and Ling Shao. Ptv2: Improved baselines with pyramid vision transformer. *arXiv preprint arXiv:2106.13797*, 2021. [2](#)
- [40] Wenhai Wang, Enze Xie, Xiang Li, Deng-Ping Fan, Kaitao Song, Ding Liang, Tong Lu, Ping Luo, and Ling Shao. Pyramid vision transformer: A versatile backbone for dense prediction without convolutions. *arXiv preprint arXiv:2102.12122*, 2021. [2](#)
- [41] Haiping Wu, Bin Xiao, Noel Codella, Mengchen Liu, Xiyang Dai, Lu Yuan, and Lei Zhang. Cvt: Introducing convolutions to vision transformers. *arXiv preprint arXiv:2103.15808*, 2021. [3](#)
- [42] Enze Xie, Wenhai Wang, Zhiding Yu, Anima Anandkumar, Jose M Alvarez, and Ping Luo. Segformer: Simple and efficient design for semantic segmentation with transformers. *arXiv preprint arXiv:2105.15203*, 2021. [2](#)
- [43] Huijuan Xu, Abir Das, and Kate Saenko. R-c3d: Region convolutional 3d network for temporal activity detection. In *Proceedings of the IEEE international conference on computer vision*, pages 5783–5792, 2017. [2](#), [6](#), [7](#)
- [44] Mengmeng Xu, Chen Zhao, David S Rojas, Ali Thabet, and Bernard Ghanem. G-tad: Sub-graph localization for temporal action detection. In *Proceedings of the IEEE/CVF Conference on Computer Vision and Pattern Recognition*, pages 10156–10165, 2020. [2](#)
- [45] Serena Yeung, Olga Russakovsky, Ning Jin, Mykhaylo Andriluka, Greg Mori, and Li Fei-Fei. Every moment counts: Dense detailed labeling of actions in complex videos. *International Journal of Computer Vision*, 126(2-4):375–389, 2018. [1](#), [2](#), [5](#)
- [46] Hang Zhao, Antonio Torralba, Lorenzo Torresani, and Zhicheng Yan. Hacs: Human action clips and segments dataset for recognition and temporal localization. In *Proceedings of the IEEE International Conference on Computer Vision*, pages 8668–8678, 2019. [2](#)
- [47] Daquan Zhou, Bingyi Kang, Xiaojie Jin, Linjie Yang, Xiaochen Lian, Zihang Jiang, Qibin Hou, and Jiashi Feng. Deepvit: Towards deeper vision transformer. *arXiv preprint arXiv:2103.11886*, 2021. [2](#)
- [48] Xingyi Zhou, Dequan Wang, and Philipp Krähenbühl. Objects as points. *arXiv preprint arXiv:1904.07850*, 2019. [5](#)
- [49] Xizhou Zhu, Weijie Su, Lewei Lu, Bin Li, Xiaogang Wang, and Jifeng Dai. Deformable detr: Deformable transformers for end-to-end object detection. *arXiv preprint arXiv:2010.04159*, 2020. [1](#), [2](#)